Available online at www.sciencedirect.com
SCIENCE DIRECT®
Journal of Power Sources 130 (2004) 266–274
JOURNAL OF POWER SOURCES
www.elsevier.com/locate/jpowsour

# Rapid test and non-linear model characterisation of solid-state lithium-ion batteries

Suleiman Abu-Sharkh, Dennis Doerffel*

*School of Engineering Science, University of Southampton, Highfield, Southampton SO17 1BJ, UK*

Received 1 August 2003; received in revised form 24 November 2003; accepted 1 December 2003

**Abstract**

This paper describes a rapid test-procedure that can be used to derive parameters of a proposed battery model. The battery model is a non-linear dynamic equivalent circuit model, which is based on Randle's model for electrochemical impedance [J. Power Sources 54 (1995) 393]. The level of sophistication has been selected such that it gives a satisfactory prediction of battery performance, but simple enough to enable on-line identification and adaptation of model parameters based on measurements of terminal voltage, current and temperature during usage. The paper also presents test data for a commercial 100 Ah battery including ageing effects.


*Keywords:* Rapid test; Lithium-ion batteries; Ageing effects

## 1. Introduction

High-energy density solid-state lithium-ion batteries are increasingly used in many applications ranging from low-power mobile telephones to high-power traction. The recent availability of high-energy cells has created new opportunities for automotive applications including electric and hybrid electric vehicles, which benefit from the high-energy density of this type of battery [2]. However, despite promising a better performance than lead acid, the younger lithium-ion technology is less well-understood and lacking information about lifetime experience.

A good battery model that relates the terminal voltage to state of charge (SOC), current, temperature and history of usage and incorporates safe operating limits should ideally be available to the designer of the system for the purpose of sizing and for the design of the battery management system that controls the charge and discharge of the battery and provides information to the user about the state of charge state of health and state of function. Ideally, such a model would have an adaptive mechanism that changes model parameters in accordance with the change of behaviour due to lifetime degradation. The parameters of a battery model are normally determined by performing charge and discharge tests under controlled conditions and monitoring terminal voltage, current and temperature.

Several different models exist for batteries. Electrochemical models and equations are normally used to design the battery, mathematical or circuit models are used to simulate battery behaviour and thermal models help designing the thermal management and predicting the thermal power limitations. Many other models are also available and usually a combination of them is required to understand the behaviour of the battery up to the required level. "Thermo Analytics Inc." [3] gives a concise and general overview of available models. Preferably the model should be as simple as possible but precise enough for the given problem, target group or application.

A simple equivalent circuit model comprising an electromotive force (emf), that can be a function of the state of charge, in series with internal resistance, which can be a function of SOC, temperature and history, may not be satisfactory in many applications. Such a model does not represent the dynamic behaviour of the battery, which in many applications is important. A dynamic model of a battery normally contains one *RC* combination like Randle's model [1] or two *RC* combinations as suggested by Gao [4] for a Sony Li-ion cell. However, many of the models published in the literature [1,4,5] assume linearity even though the actual behaviour of the battery is found to be significantly non-linear.

The open-circuit voltage (OCV) is one of the most important parameters of a battery. In a conventional test, this voltage is normally measured as the steady-state open-circuit

* Corresponding author. Tel.: +44-2380-592698; fax: +44-23-8049-3053.
*E-mail address:* ddoerffel@ses.soton.ac.uk (D. Doerffel).

0378-7753/$ – see front matter © 2004 Elsevier B.V. All rights reserved.
doi:10.1016/j.jpowsour.2003.12.001

terminal voltage at different states of charge. However, for each of state of charge this measurement can take a long time. Preliminary tests on our test candidate have indicated that the steady-state is reached after a time of the order of 24 h. Such a test would take days to perform on a single cell. If the cell chemistry shows a voltage hysteresis between charging and discharging, as it is the case for NiMH batteries for example [6], it would take 20 days in order to determine the OCV. Additional tests are required for determining other battery model parameters like the mentioned *RC* combinations for example. All parameters usually vary with state of charge, temperature, age and history (number and depth of cycle) of the cell not to mention variations between cells due to manufacturing tolerances. These costly time-consuming tests are not suited for in situ parameter identification and they are in contrast with the actual rapid battery development.

This paper describes a rapid test-procedure that can be used to derive parameters of a proposed battery model. The battery model is a non-linear dynamic equivalent circuit model that is based on Randle's model for electrochemical impedance. The level of sophistication has been selected such that it gives a satisfactory prediction of battery performance, but simple enough to enable on-line identification and adaptation of model parameters based on measurements of terminal voltage, current and temperature during usage. The paper also presents test data for a commercial battery.

## 2. Experimental apparatus

The tests were carried out on a Digatron universal battery tester (UBT) 100-18-6 at the Institute for Power Electronics and Electrical Drives (ISEA) in Aachen, Germany. The UBT 100-18-6 is capable of charging and discharging the battery at a maximum rate of 100 A. It can operate in several modes such as constant-current and constant-voltage. It comprises voltage, current and temperature measurements and a computer interface. Table 1 summarizes the specifications of the UBT.

A high-energy solid-state lithium-ion cell with a capacity of 100 Ah was tested. The cell remained within the battery block during the tests to represent a typical in-vehicle configuration. The test arrangement is shown in Fig. 1. The third cell was chosen for testing, because other cells surround it and this is the worst case in terms of temperature rise during high-current discharge and charge. The battery was placed on a plastic grid to allow for natural air-cooling and for isolating the battery from the "ground" heatsink, so that the cell heats up uniformly during the test. The ambient air temperature was 21 °C during the tests.

Table 1
Specifications of the Digatron UBT 100-18-6 universal battery tester

| | |
|---|---|
| Maximum discharging current (A) | 100 |
| Maximum charging current (A) | 100 |
| Voltage range during charging (V) | 1–18 |
| Voltage range during discharging (V) | 0–15 |
| Error (current measurement) (mA) | ±0.5% but not better than ±50 |
| Error (voltage measurement) (mV) | ±5 |
| Error (temperature measurement) (K) | ±0.1 |

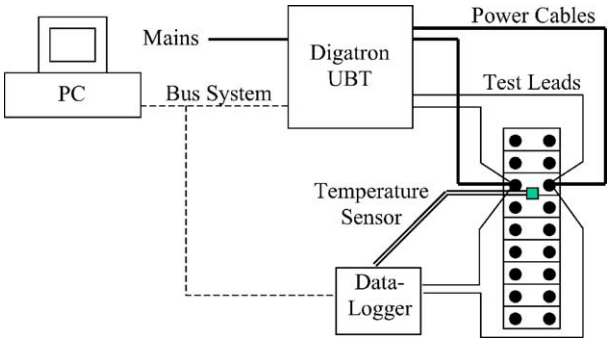


Fig. 1. Arrangement for testing the Li-ion battery on the Digatron battery tester.

The battery tester was connected to the cell using cables with 10-mm$^2$ cross-section. The test leads for measuring the cell-voltage are separate from the power cables to eliminate errors due to cable voltage drop. A data-logger (Digatron DLP 24C) was used to verify voltage measurement of the battery tester and for measuring cell temperature. The temperature probe was placed between cell three and cell four. The battery tester and the data-logger are connected to a PC through a bus system.

## 3. Test-procedure

The software "Digatron BTS 600" allows programming the test-procedure and logging data like time, current, voltages, power, temperature, watt-hours and ampere-hours. The sampling time and start/stop criteria can be programmed. Several limits for the battery can be defined separately, so that the tester will stop for safety reasons in case these values are reached.

The tested battery was new and it had to be cycled before starting the test. The behaviour was stable after the first cycle. Fig. 2 shows the first two test cycles. The test starts with a pause of 1 min in order to measure the initial voltage of the cell. The battery is charged with the rated current or less (33 A in our case) till it reaches the maximum charging voltage (4.2 V in our case). Charging continues at this voltage and the current decreases till it reaches the charge-termination current (1.1 A in our case). The manufacturer specifies this as the fully charged condition. After pausing for 1 h, the battery is discharged with a current of 33 A. It is depleted once it reaches 2.8 V at this current. The discharging/charging procedure is repeated a second time after waiting for 1 h. The first cycle assures reaching a certain battery condition. The status of a cell is usually unknown and cycling it once with a defined waiting time before starting

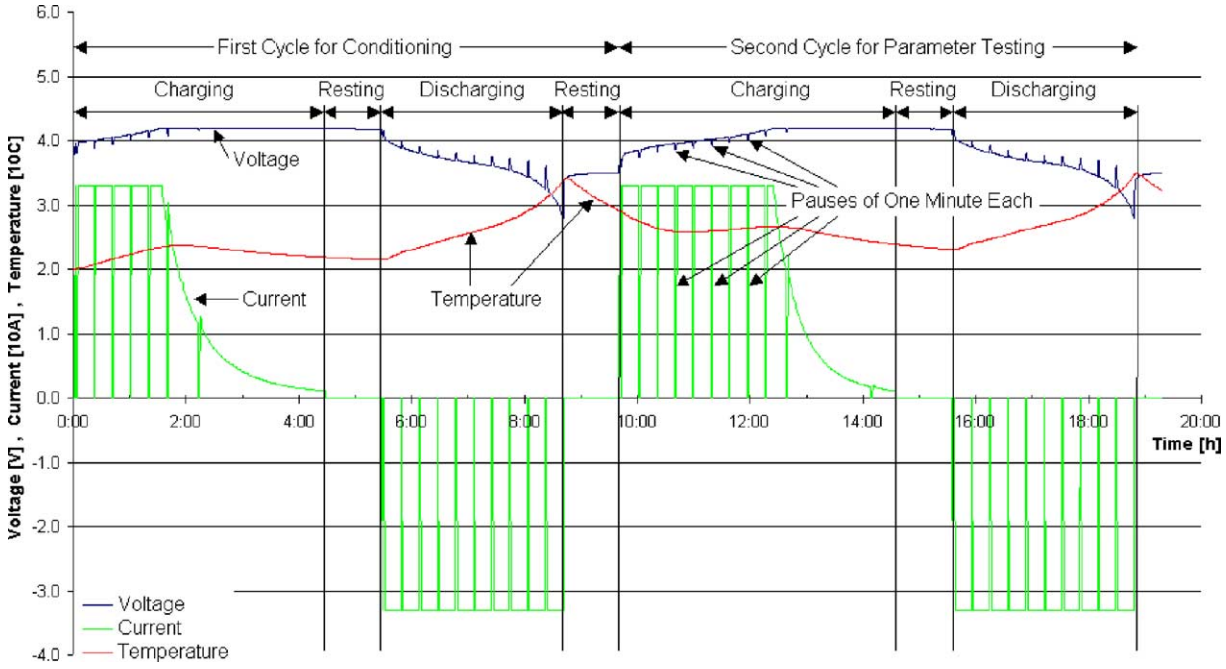


Fig. 2. Typical test curves for a 100 Ah Li-ion battery.

the actual test assures comparable test-conditions. The second cycle is used for determining battery model parameters.

The discharging and the charging process is paused after the first 1 Ah and then every 10 Ah in order to record and analyse the dynamic behaviour of the battery at different SOC. A rest of 1 h is always applied between charging and discharging. This allows the battery to approach equilibrium and to cool down. Measurements are taken every 2 mV change of cell-voltage or additionally every change of 0.5 A change in current (during charging only). This setting keeps the number of data small when no changes occur and takes faster measurement when rapid changes take place. It ensures reliable measurements in constant-current and constant-voltage phases. The measurements of cell-voltage

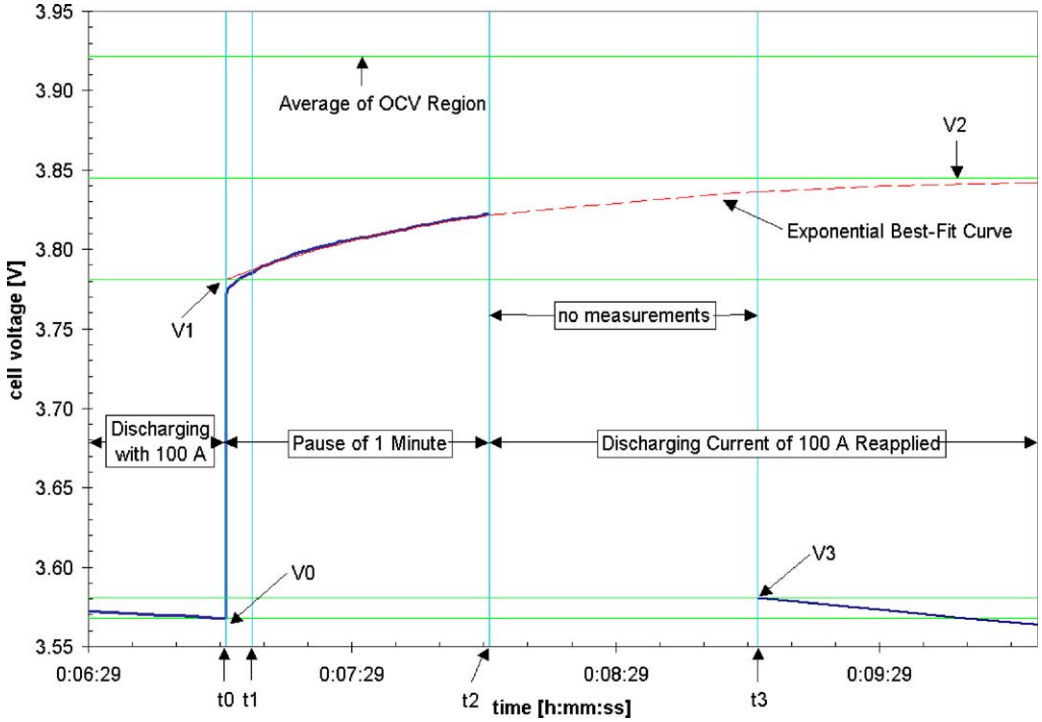


Fig. 3. Dynamic behaviour of cell-voltage when pausing the 100 A discharge current at a SOC of 71 Ah.

(direct), cell-voltage (through data-logger), current and temperature are recorded. Accumulated data like Ah and Wh are also recorded in total (balanced counting), per step and for charging in total and discharging in total.

Fig. 2 shows typical voltage, current and temperature curves that were obtained from these tests. Charging current is shown positive and discharging current is shown negative. The temperature and the current are scaled with a factor of 10 on the *y*-axis. Fig. 3 shows a typical cell-voltage during a discharge pause period (it is an expanded part of a voltage curve in Fig. 2). This figure will be studied in more detail later in this paper.

## 4. Non-linear dynamic battery model

Fig. 4 shows the proposed equivalent circuit model for the tested solid-state lithium-ion cell during discharge. The model for charging is equivalent to this one, but with the zener-diode the other way round. The OCV or emf is modelled as an ideal voltage source that is a function of the SOC.

$R_p$ models the self-discharge rate, which is related to the electronic conductivity of the electrolyte. This is of interest for predicting the state of charge in case the cell is not used for a long time. It has been suggested that lithium-ion batteries require cell-balancing in order to offset variations in self-discharge rates, because they cannot be equalised based on a small controlled overcharge [7]. These variations in self-discharge rates need to be considered when designing cell-equalisation systems.

The zener-diode and the time-constant of $R_{long}C_{long}$ model a constant-voltage drop, which has been observed during tests. The delay time caused by $R_{long}C_{long}$ is in the order of several hours. Future research has to show whether this part of the model can be related to diffusion limitations in this Li-ion cell with colloidal gel-type electrolyte. The simplicity of this part of the model enables determination of SOC based on terminal voltage measurement. Knowing $R_{long}$ is essential for predicting the behaviour at low-currents like small stand-by loads or equalising currents, because $R_{long}$ is much higher than $R_{01}$ and it determines the voltage drop at low-currents.

The second *RC* combination with $R_{12}$ and $C_{12}$ models the double-layer capacitance and the reaction kinetics. It explains the exponential rise of the terminal voltage between $t_1$ and $t_2$ in Fig. 3. It determines the dynamic behaviour of the battery during power bursts, like for example during regenerative braking in vehicles. The time-constant is in the order of 1 min.

$R_{01}$ is the total Ohmic resistances in the cell, like terminal resistances and current collector resistances. The immediate voltage rise between $V_0$ and $V_1$ in Fig. 3 is due to this resistor. It is responsible for power-capability, because it causes the biggest share of the total voltage drop at high currents.

## 5. Analysis of test data—OCV

The following sections discuss the methods used to determine model parameters from the test-procedure shown in Figs. 2 and 3. Two different methods for determining the OCV are investigated. The first method is based on measured values only and the second method makes use of exponential curve fitting and extrapolation.

### 5.1. First method

To determine the open-circuit voltage of the battery, the results in Fig. 2, are re-plotted as shown in Fig. 5 in which the voltage during the described test-procedure is plotted against the SOC of the battery.

In Fig. 5, the voltage drops at 1 Ah and every 10 Ah that can be seen during charging are caused by the pauses of 1 min as defined in the test-procedure. On discharge the voltage rises during these pauses. All voltages reached during the pauses at different SOC during discharging and charging are connected with the dotted line. These dotted curves for charge and discharge would be expected to be identical, representing the OCV, if the pauses were long enough (of the order of 24 h). However, in this case, they are not identical,

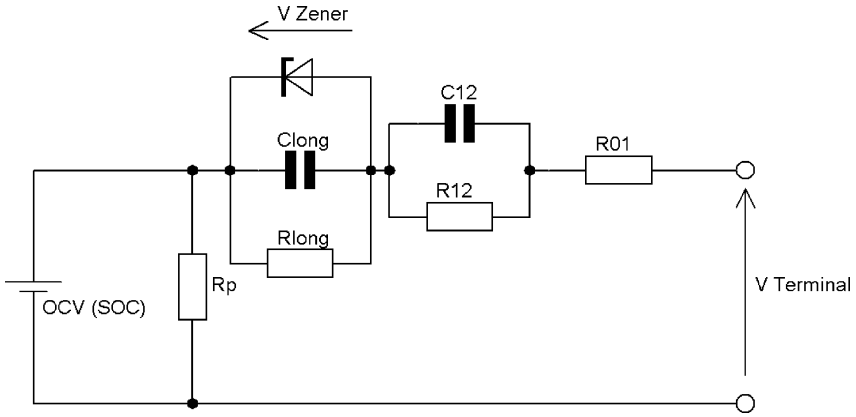


Fig. 4. Proposed equivalent circuit model for the solid-state Li-ion cell during discharge.

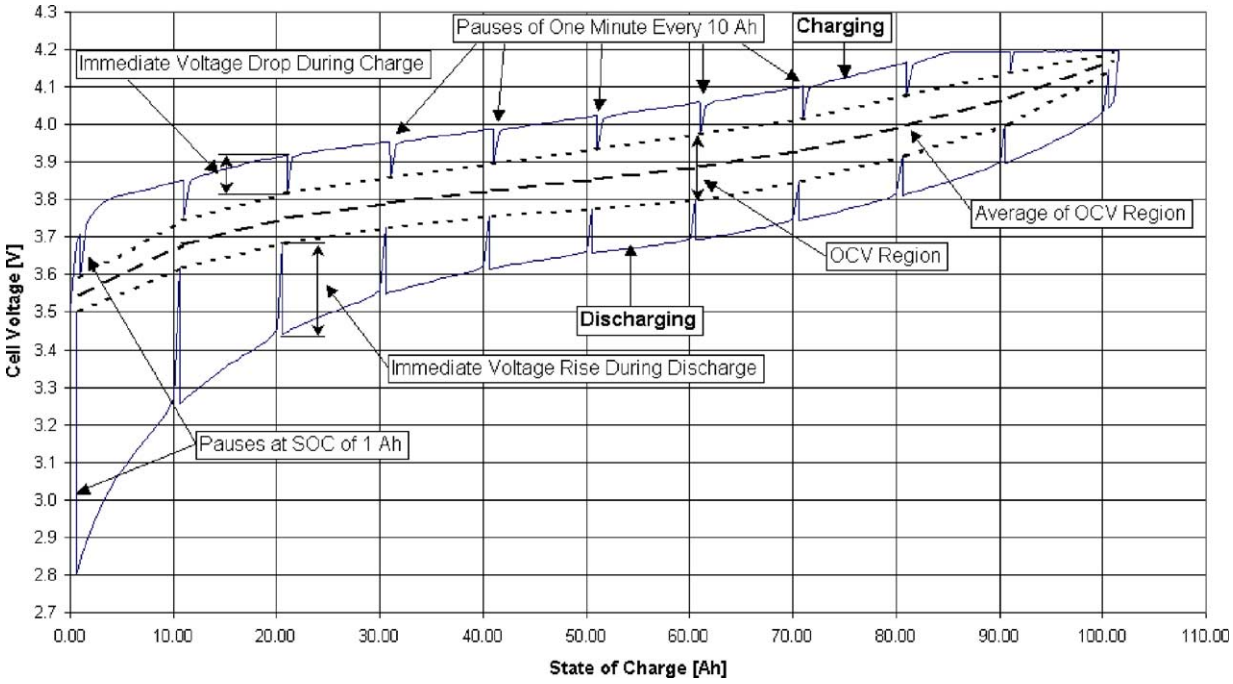


Fig. 5. Cell-voltage vs. SOC during charging and discharging.

which can be explained by the fact that the cell did not reach steady-states during the 1-min pauses. The OCV cannot be measured directly, but it is assumed that the area between the two dotted lines is the region where the OCV can be found. The dashed line shown in Fig. 5 is the mean of the dotted lines. For validation reasons only, the described test has been repeated based on a higher charging and discharging current (100 A instead of 33 A). The same analysis is applied and the resulting dashed mean curve matches the one obtained from the 33 A test with an error of less than ±10 mV or ±1.5% of SOC.

### 5.2. Second method

This method is based on using the data shown in Fig. 3. The first 30 s in this figure show the cell being discharged with 100 A till time $t_0$. During this discharge period the cell terminal voltage decreases towards the level of $V_0$ with decreasing SOC. The load is switched off at $t_0$ and the voltage rises almost immediately to the level of $V_1$. During the pause of 1 min between $t_0$ and $t_2$ the voltage seems to rise exponentially. The discharging current is reapplied at $t_2$ and the next measurement is taken 1 min later at $t_3$ where the voltage has dropped down to $V_3$.

Fig. 3 shows how an exponential best-fit curve has been laid over the measurement during the pause period. The time between $t_0$ and $t_1$ (5 s) has not been taken into account when searching for this best-fit, because the time-constant in the first seconds is much shorter. Good correspondence between the curve-fit and actual measurement data could be found by omitting these first 5 s. The level $V_2$ is the extrapolated steady-state value of the best-fit exponential curve. It defines the upper limit of the OCV region during charging and it defines the lower limit during discharging. The mean value of $V_2$ during charging and discharging is the OCV proposed in this second method. The results of different OCV test-methods are presented in Fig. 6 for comparison. The curves for different test-methods and currents are almost indistinguishable, which shows that the two methods produce almost identical results.

In Fig. 6, no measurements were taken at low SOC at 100 A, because the battery tester configuration was not suitable for this test condition. There are slight differences of about ±10 mV between the tests with different currents at SOC of 80 and 90%. The results from the first method and the second method on the other hand are coincident. It is sufficient to make use of the simpler first method for determining OCV. It is not necessary to employ exponential regression as proposed in the second method.

The following paragraphs investigate, whether the OCV results from the rapid method described above agree with results obtained from conventional test-method with long waiting time. A test with a waiting time of 12 h at each SOC level has been carried out. The battery has aged for 1 year and some cycles in an electric vehicle between the proposed test and the conventional test. The total available capacity went down from 101 to 94 Ah under same test conditions. A first analysis was based on a diagram showing the OCV as a function of SOC in Ah. This diagram revealed unsatisfactory results, because of the Ah shift. The diagram in Fig. 7 presents and compares the results using SOC in percentage as *x*-axis.

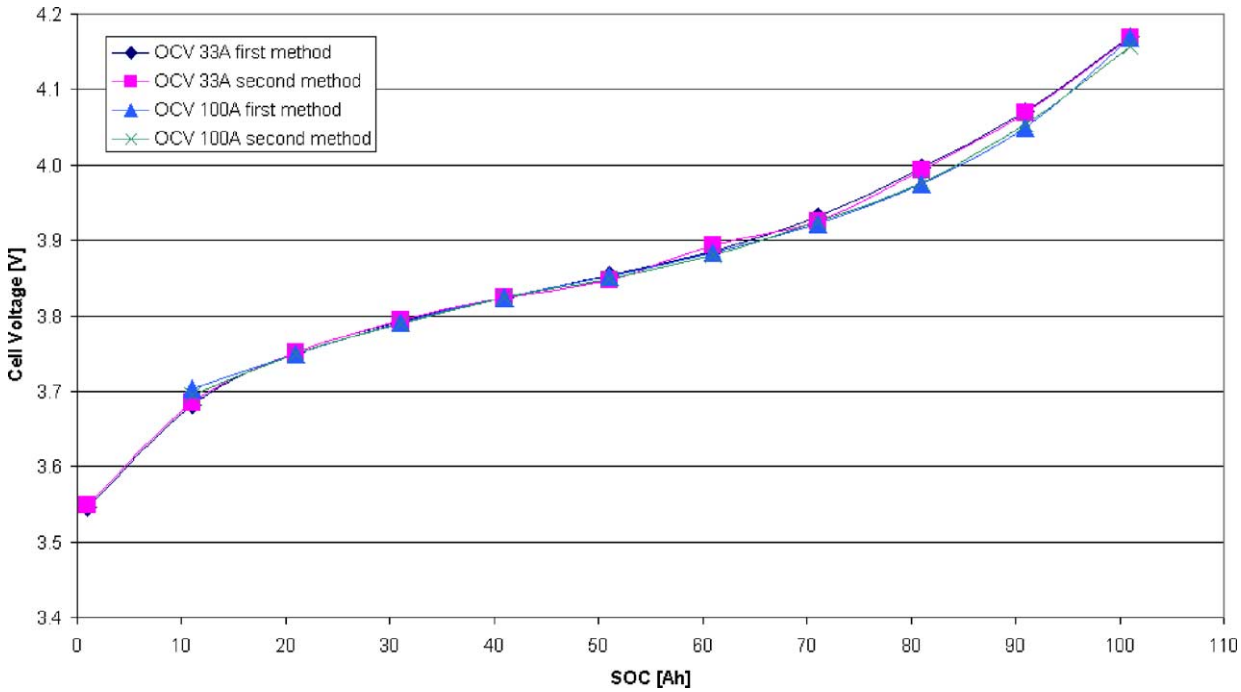


Fig. 6. OCV vs. SOC curves obtained from different methods.

Fig. 7 shows the OCV region obtained from the proposed rapid test. The region is between the top curves obtained during charging and the bottom curves obtained during discharging. The curves between using the same colour and pattern represent the mean values between charging and discharging. The two black curves in the middle represent the OCV results obtained from the long-term test with a waiting time of 12 h. The top one is for charging and the bottom one for discharging. The long-term test has been performed on an aged battery (16 full cycles and 1-year-old), while the rapid test was performed on the same cell when it was new. The rapid test has been repeated just before the long-term

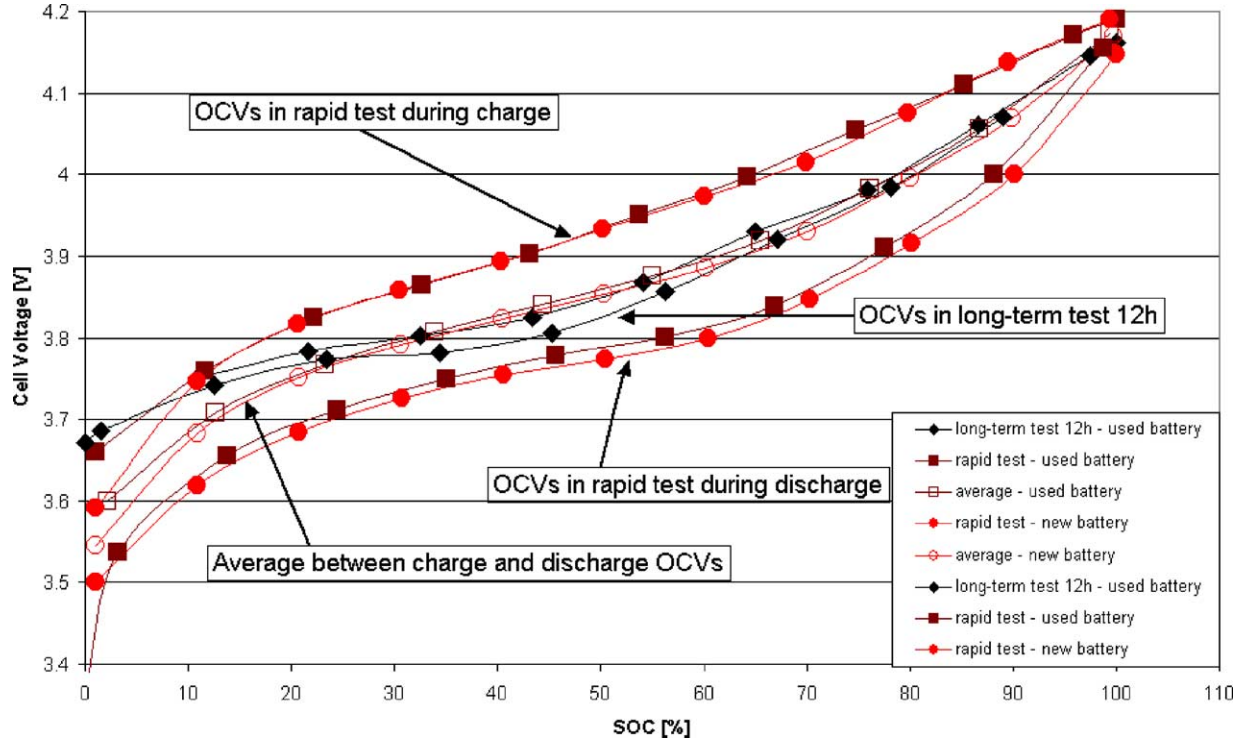


Fig. 7. Comparison of OCV obtained from different tests and different age of battery.

test in order to receive comparable results. The red curve with the dots represents the test with the new battery and the brown curve with the squares represents the used battery.

It can be seen that the battery age has only marginal influence on the shape of the OCV curves if plotted against the SOC expressed in percentage. The two curves obtained from the long-term test do not match between charging and discharging. This reveals that even a waiting time of 12 h is not sufficient to fully reach equilibrium. The OCV results from the proposed rapid test-method match the results from the long-term test reasonably well between 20 and 100% SOC. They are lower at SOC levels below 20%. This can be explained by the short waiting time between discharging in the first cycle and charging in the test cycle as shown in Fig. 2. Another factor is that during discharge, concentration gradients build up by, which cannot be offset during the first minutes of charging due to slow mass transport in the gelled electrolyte and voltage drop is more noticeable at low (local) SOC thanks to the reaction kinetics. This problem is not noticeable at full charge, because the current reaches small values at the end of charge, whereas current remains high during discharge till cell-voltage is 2.8 V.

This paragraph has shown, that the proposed rapid method is suitable for determining the OCV between 20 and 100% SOC. The first simpler method is sufficient for OCV determination, whereas the following paragraph will rely on the second method using exponential extrapolation in order to determine dynamic model parameters.

## 6. Analysis of test data—dynamic behaviour

The following paragraphs investigate the dynamic behaviour of the cell. The battery model parameters will be determined based on the test explained earlier. The battery was naturally cooled, and therefore, the cell temperature was not constant. It was varying as shown in Fig. 2. This will enable us to make some qualitative statements on the temperature dependency of model parameters.

With reference to Fig. 3, the instantaneous voltage rise when the discharging stops is defined as:

$$\Delta V_{01} = |V_1 - V_0|$$

It is assumed that this immediate voltage drop can be related to the internal Ohmic resistance $R_{01}$ of the battery. This resistance can be calculated for charging and for discharging at various SOC, based on the following equation:

$$R_{01} = \frac{\Delta V_{01}}{|I|}$$

Fig. 8 shows the result of this analysis. The two top curves show the resistance $R_{01}$ during discharging as a function of SOC. One is obtained from the 33 A test and the other from the 100 A test. The two other curves show the equivalent but during charging. In general, the resistance is lower at higher currents. The charge resistance is lower than the discharge resistance.

Similarly, the other resistances in the circuit model can be determined using the following equations:

$$\Delta V_{12} = |V_2 - V_1|$$

$$R_{12} = \frac{\Delta V_{12}}{|I|}$$

Fig. 9 shows the resistance $R_{12}$ as a function of SOC during discharging and charging with 33 and 100 A. The scale on the *y*-axis is the same as in Fig. 8 for better comparison. The curves are almost indistinguishable in this scale and

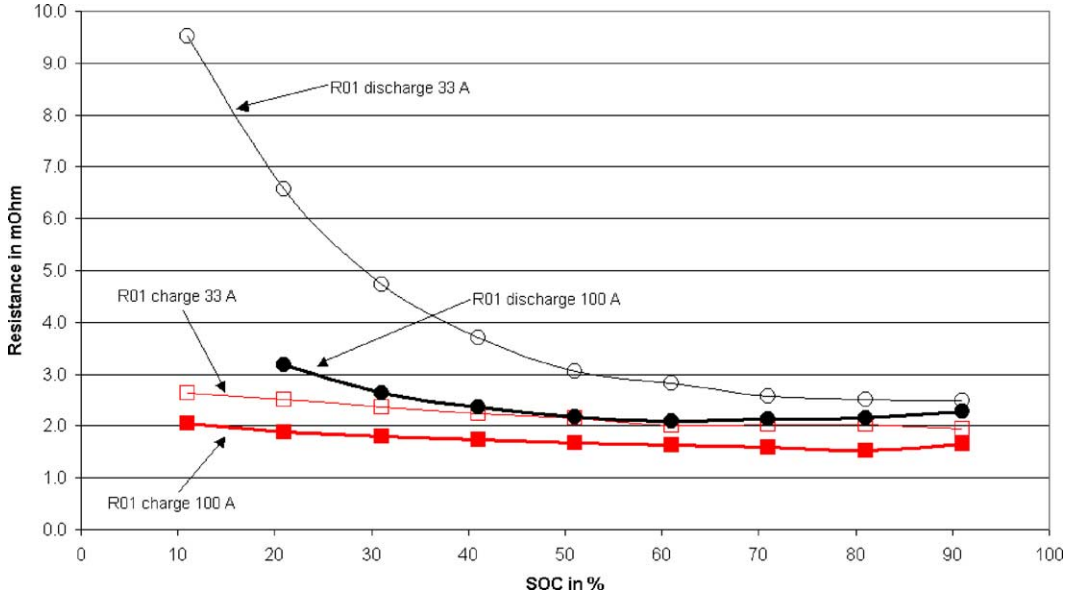


Fig. 8. Internal resistance $R_{01}$ as a function of SOC during charging and discharging obtained from different tests (temperature not constant).

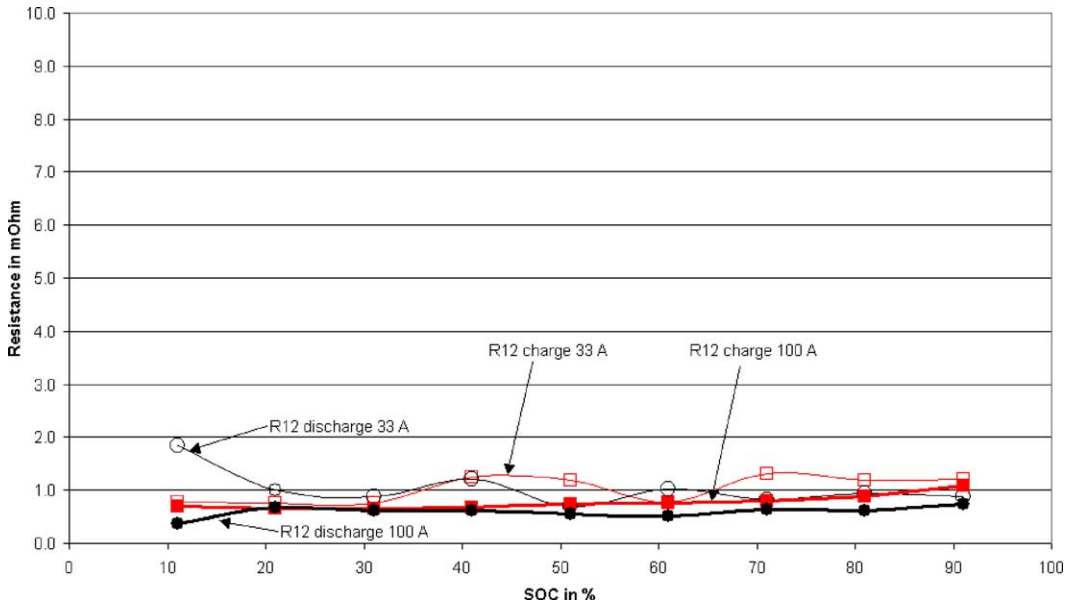


Fig. 9. Internal resistance $R_{12}$ as a function of SOC during charging and discharging with 33 and 100 A (temperature not constant).

remain almost constant throughout different SOCs if compared with the generally higher values of $R_{01}$ in Fig. 8. The results do not show any significant trend within the SOC range or any significant dependency on the current. Resistance during charging and discharging are similar. The temperature varied between 23 and 45 °C during tests, but $R_{12}$ shows no relation to these temperature changes. In conclusion, $R_{12}$ can be called constant if compared with $R_{01}$. The calculated mean value of $R_{12}$ is 0.869 mΩ with a standard deviation of 0.277 mΩ.

The last analysis focuses on the voltage difference between $V_2$ and the average of the OCV region. The average of the OCV region will be called OCV in the following text. Though the graph in Fig. 3 suggests that the cell-voltage approaches level $V_2$, additional tests have revealed that it actually approaches OCV, if waited for long enough.

Fig. 10 shows the level $V_2$ for charging and discharging, at 33 and 100 A and the OCV over SOC. It reveals that the level of $V_2$ is independent on the current. The difference between $V_2$ and OCV for SOC levels between 10 and 90% is a constant 68 mV measured with a standard deviation of 12 mV. This difference is the same for charging and discharging and shows no relation to the temperature changes during tests. It is sensible to model this voltage drop with a zener-diode instead of using a resistor, because the voltage drop is constant and not proportional to the current.

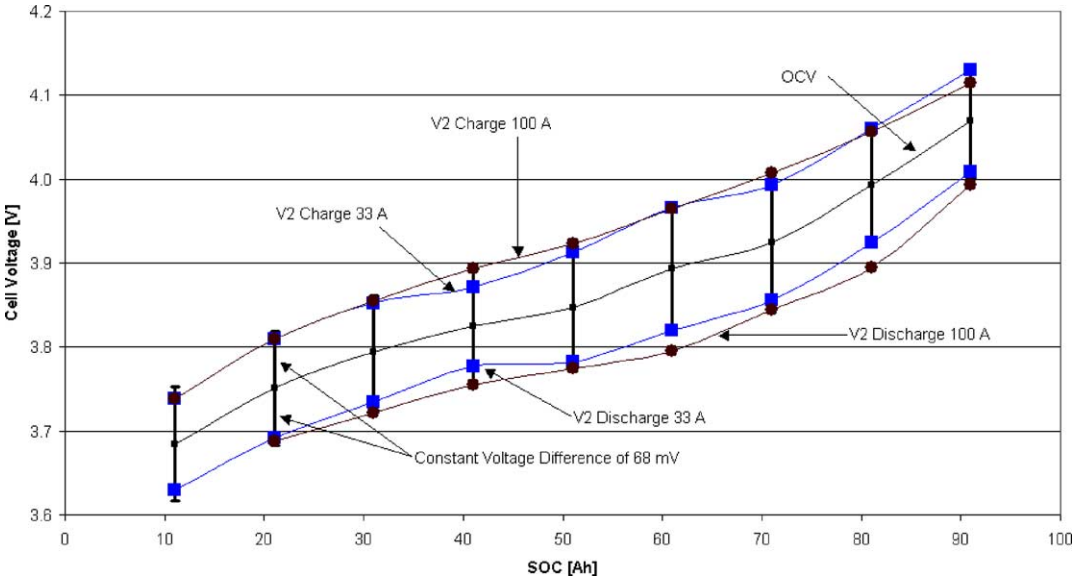


Fig. 10. $V_2$ during charge and discharge at 33 and at 100 A and OCV over SOC.

## 7. Discussion and conclusions

A non-linear dynamic equivalent electrical circuit model for a high-energy lithium-ion battery has been presented. The dynamic behaviour is modelled using two *RC* combinations and the non-linearity is modelled using a zener-diode. The value of the zener-diode is constant between 10 and 90% SOC, it is independent of the temperature and ageing did not show an effect to it so far (1 year and 16 cycles). The deviation of the results is acceptable. One *RC* combination represents a very long time-constant in the order of several hours. This is related to the constant-voltage drop of the zener-diode. The second *RC* combination represents another time-constant in the order of minutes. The voltage drop related to this time-constant is proportional to the current and is modelled with the resistor $R_{12}$. This resistor is almost constant between 10 and 90% SOC and similar between charging and discharging. It is independent on the temperature, but the deviation of the results is quite high. This suggests that the model or the test require improvements. On the other hand $R_{12}$ values are small if compared with voltage drops due to $R_{01}$ and the zener-diode. This means that the deviation has a small impact on the overall model. The immediate voltage drop has been modelled with the resistor $R_{01}$. $R_{01}$ is not constant over the SOC range, nor is it constant with the current. It is likely that it is temperature dependent as well. $R_{01}$ and the dependencies require further testing and analysis. Fortunately $R_{01}$ can be measured using fast methods like impedance spectroscopy [1]. On the other hand, the actual model will require look-up tables or multi-dimensional functions or graphs to determine $R_{01}$ as a function of current, temperature and age. This is not ideal and the model may require improvement in order to get simpler dependencies. The self-discharge rate is modelled with $R_p$, which has not been determined yet. The OCV is represented as a function of the SOC. It appears to be independent on the age of the battery.

A rapid test-method has been presented. It helps determining the parameters of the model except the self-discharge rate $R_p$ in less than 19 h per cell. The OCV can be determined with reasonable accuracy between 20 and 100% SOC without waiting for equilibrium. Waiting times of less than 1 min are sufficient if the average between charging and discharging is taken. The OCV at levels below 20% SOC cannot be determined using this method. The proposed test-method reduces the time for testing from almost 20 days to less than 19 h per cell. Further investigations are required to determine the dynamic behaviour not only after stopping the current but also when applying a current. The resistor $R_{long}$ needs to be determined by additional tests, because it is of interest for small currents and equalisation requirements. The capacitors do not need to be determined. The time-constants are sufficient for most applications. It is sufficient to know whether they are in the order of seconds, minutes, hours or days and this can extracted from the proposed test-method.

Future work will focus on validating the proposed battery model by applying different test-methods such as impedance spectroscopy and by comparing different analysis such as Nyquist plots and Lissajous plots. The model will then be assessed by comparing simulation results with in-vehicle testing, before it can be implemented for in-vehicle life-time assessment that aims to reveal parameter dependencies on age, cycles and temperature. Once the model is valid and applicable, the test-procedures can be optimised.

## Acknowledgements

The authors would like to thank Institute for Power Electronics and Electrical Machines (ISEA, Aachen, Germany) for using their battery tester, also S. Buller and O. Bohlen from ISEA for help with the testers and Professor Alan Ward and Professor Honor Ward for proof-reading.

## References

[1] P. Baudry, M. Neri, M. Gueguen, G. Lonchampt, J. Power Sources 54 (1995) 393–396.
[2] D. Doerffel, S. Abu-Sharkh, in: Proceedings of 19th Electric Vehicle Symposium, 2002, EVAAP (Electric Vehicle Association of Asia Pacific).
[3] Thermo_Analytics_Inc. (available from: http://www.thermoanalytics.com) accessed on 1 June 2003.
[4] L. Gao, IEEE Trans. Components Packag. Technol. 25 (2002) 495–505.
[5] Y.-S. Lee, J. Wang, T.-Y. Kuo, in: Proceedings of 19th Electric Vehicle Symposium, 2002, EVAAP (Electric Vehicle Association of Asia Pacific).
[6] C.G. Motloch, G. Hunt, J.R. Belt, C.K. Ashton, G.H. Cole, T.J. Miller, C. Coates, H.S. Tataria, G.E. Lucas, T.Q. Duong, J.A. Barnes, R.A. Sutula, in: Proceedings of 19th Electric Vehicle Symposium, 2002, EVAAP (Electric Vehicle Association of Asia Pacific).
[7] S.W. Moore, J. Schneider, in: Proceedings of SAE Technical Paper Series, 2001, http://www.SAE.org (Society of Automotive Engineers).